NASA

MEMORANDUM

HEAT TRANSFER IN THE TURBULENT INCOMPRESSIBLE BOUNDARY LAYER

I - CONSTANT WALL TEMPERATURE

By W. C. Reynolds, W. M. Kays, and S. J. Kline
Stanford University

NATIONAL AERONAUTICS AND SPACE ADMINISTRATION
WASHINGTON
December 1958

NATIONAL AERONAUTICS AND SPACE ADMINISTRATION

MEMORANDUM 12-1-58W

HEAT TRANSFER IN THE TURBULENT INCOMPRESSIBLE BOUNDARY LAYER

I - CONSTANT WALL TEMPERATURE

By W. C. Reynolds, W. M. Kays, and S. J. Kline

SUMMARY

Heat-transfer rates, velocity profiles, and temperature profiles for the turbulent incompressible flow of air over a flat plate with a constant surface temperature have been measured at Reynolds numbers up to 3.5×10^6. The turbulent heat-transfer measurements agree well with the von Kármán analogy, and the velocity profiles agree with the data of previous investigators. The temperature profiles are similar to the velocity profiles, both being adequately described by power formulas.

INTRODUCTION

The present report is the first of a series of four covering a three-year investigation of heat transfer in the turbulent incompressible boundary layer with arbitrary surface temperature (see ref. 1). In this report the experimental apparatus is described and the results of experiments with constant surface temperature are presented. Part II contains experimental results and analyses for a step temperature distribution (ref. 2). In part III the step-function analysis is used to predict heat-transfer rates for several variable-wall-temperature cases, and the predictions are compared with experiment (ref. 3). A simple method for handling variable-surface-temperature problems is presented. The effect of the location of transition on the heat transfer in the turbulent boundary layer is analyzed and compared with experiments in part IV (ref. 4).

The broad objectives of this program were to investigate experimentally the problems of heat transfer in a turbulent incompressible boundary layer on a flat plate, with negligible pressure gradient, at high Reynolds numbers. The Mach number and temperature difference are sufficiently low that compressibility effects are negligible, and temperature-dependent fluid-property effects are small. This is a problem that has been extensively investigated analytically, but adequate experimental confirmation of the analyses was lacking.

This first report treats the problem of heat transfer from a flat plate at constant wall temperature. A number of analyses for the heat-transfer rate have been proposed, and some experiments have been performed. However, the only reliable data at Reynolds numbers over about 5×10^5 have been obtained at high velocities, where compressibility effects are important. Thus, there is a need for experimental confirmation of the analyses, and the constant-surface-temperature data contained in this report are presented primarily for purposes of this confirmation. They also form a point of departure for the work described in the subsequent reports.

Perhaps the best analysis available at the present time is the heat-transfer - momentum analogy of von Kármán (ref. 5), by which the local heat-transfer coefficient has been related to the local friction factor. A suitable expression for the friction factor in terms of the local Reynolds number is then required. A number of analyses for friction factor are available, and that of Schultz-Grunow (ref. 6) has been experimentally verified over a wide range of Reynolds numbers. The von Kármán analogy, combined with the friction-factor formula of Schultz-Grunow, allows prediction of the local heat transfer. This result is in excellent agreement with the experimental data to be presented in this report at flow Reynolds numbers from 10^5 to 3.5×10^6.

An alternative method of analyzing skin friction and heat transfer is to assume the form of the velocity and temperature profiles, and then to use the momentum and energy integral equations of the boundary layer to arrive at expressions for the friction factor and heat-transfer coefficient as functions of the local Reynolds number. In making such analyses it is convenient to represent the profiles by power expressions, and it is commonly assumed that velocity and temperature vary as the one-seventh power of the distance from the surface. The data of Schultz-Grunow indicate that the 1/7-power velocity profile is reasonable at Reynolds numbers near 10^7 but is not accurate for lower or higher Reynolds numbers (ref. 6). Velocity profiles obtained in the present investigation agree quite well with the Schultz-Grunow profiles; the temperature profiles obtained at constant wall temperature are indeed "similar" to the velocity profiles, both being described very well by 1/5.6-power formulas. The survey data presented in this report are therefore of interest because they may be used as the basis for integral analyses for friction and heat transfer in the turbulent boundary layer.

This investigation was carried out at Stanford University under the sponsorship and with the financial assistance of the National Advisory Committee for Aeronautics. The assistance of the following people is gratefully acknowledged: H. M. Satterlee designed the experimental apparatus and supervised the construction with B. J. Grotz, who constructed the instrumentation and assisted in some of the preliminary tests.

P. W. Rundstadler, R. M. Foster, J. D. Stephenson, G. L. Meyers, and M. L. van der Ploeg assisted in the wind-tunnel testing, and L. R. Reneau and H. Singh reduced the bulk of the data.

SYMBOLS

C_f friction factor, $\tau_w/(\rho u_\infty^2/2)$

C_p pressure coefficient, $(p - p_s)/(p_t - p_s)$

c_p specific heat at constant pressure, Btu/(lb)(°F)

G free-stream mass velocity, ρu_∞, lb/(hr)(sq ft)

h convective heat-transfer coefficient, $q_w''/\Delta t$, Btu/(hr)(sq ft)(°F)

k thermal conductivity of fluid, Btu/(hr)(ft)(°F)

Pr Prandtl number, $\mu c_p/k$

p pressure, lb/sq ft

p_s static pressure upstream of plate, lb/sq ft

p_t total pressure upstream of plate, lb/sq ft

q_{bl}'' heat flux in boundary layer, Btu/(hr)(sq ft)

q_w'' heat flux at wall, Btu/(hr)(sq ft)

Re_x flow Reynolds number, Gx/μ

Re_δ Reynolds number based on δ, $G\delta/\mu$

St local Stanton number, h/Gc_p

T_w absolute wall temperature, °R

T_∞ absolute free-stream temperature, °R

Δt $t_w - t_\infty$, °F

t_{bl} temperature in boundary layer, °F

t_m mean temperature of heated strip, °F

Δt_m	$t_m - t_\infty$, °F
t_w	wall temperature, °F
t_∞	free-stream temperature, °F
t^+	dimensionless temperature, $(t_w - t_{bl})\rho c_p\sqrt{\tau_w/\rho}/q''_w$
u	velocity in x-direction, ft/sec
u_∞	free-stream velocity, ft/sec
u^+	dimensionless velocity, $u/\sqrt{\tau_w/\rho}$
v	velocity in y-direction, ft/sec
x	distance from leading edge, ft
y	distance from plate, ft
y^+	dimensionless distance from wall, $y\sqrt{\tau_w/\rho}/\nu$
α	thermal diffusivity of fluid, sq ft/hr
δ	thickness of hydrodynamic boundary layer, ft
δ^*	displacement thickness, $\int_0^\delta \left[1 - (u/u_\infty)\right] dy$, ft
δ_T	thickness of thermal boundary layer, ft
δ_T^*	conduction thickness, $\int_0^{\delta_T} (1 - \theta) dy$, ft
ϵ_H	eddy diffusivity for heat, sq ft/hr
ϵ_M	eddy diffusivity for momentum, sq ft/hr
θ	dimensionless temperature, $(t_w - t_{bl})/(t_w - t_\infty)$
μ	viscosity of fluid, lb/(hr)(ft)
ν	kinematic viscosity, μ/ρ, sq ft/hr
ρ	fluid density, lb/cu ft

τ_{bl} shear stress in boundary layer, lb/sq ft

τ_w shear stress at wall, lb/sq ft

ANALYSIS

Heat Transfer

The problem of turbulent heat transfer from a flat plate has been attacked analytically by a number of investigators, generally by one of two methods. One approach is the integral method, wherein the form of the velocity and temperature profiles is assumed, and the energy integral equation is used to arrive at a relation between the local heat-transfer coefficient and the local friction factor. The integral method is very powerful, because the result is relatively insensitive to the choice of the temperature and velocity profiles. The second method is the analogy method, wherein mechanisms for heat and momentum diffusion throughout the boundary layer are assumed, and an empirical velocity profile is employed to determine the heat-transfer rate in terms of the local friction factor. The resulting expressions for the local heat-transfer coefficient are generally more complicated than those obtained by integral methods, but they agree better with experimental values.

It appears that the best analysis available at the present time is the heat-transfer - momentum analogy of von Kármán (ref. 5), who obtained

$$St = \frac{C_f/2}{1 + \sqrt{C_f/2}\left[5Pr + 5\ \ln(5Pr + 1) - 14\right]} \tag{1}$$

For Prandtl numbers of unity this result reduces to the familiar Reynolds analogy,

$$St = C_f/2 \tag{2}$$

It is evident that the friction factor must be known if the heat-transfer rates are to be determined, and a number of friction-factor analyses have been made (ref. 7). An expression for the local friction factor may be derived by integral methods, if it is assumed that the velocity profile follows a 1/7-power law and that the wall shear stress is related to the boundary-layer thickness by

$$C_f/2 = 0.0228\ Re_\delta^{-1/4} \tag{3}$$

This relation was first proposed by Blasius on the basis of pipe-flow friction data. These assumptions lead to (ref. 8)

$$C_f/2 = 0.0296\ Re_x^{-0.2} \tag{4}$$

Equation (4) appears to be adequate at Reynolds numbers below 10^6 but gives friction factors that are low above Re_x of 10^6 to 10^7. A more refined analysis was made by Schultz-Grunow, who measured velocity profiles and local friction factors at Reynolds numbers up to 10^9 (ref. 6). He then used the momentum integral equation to find the friction factor and obtained a result that may be represented by

$$C_f/2 = 1.60(\ln Re_x)^{-2.58} \tag{5}$$

Equation (5) is in good agreement with Schultz-Grunow's data for Reynolds numbers up to 10^9, and it is felt that this is the best friction-factor relation available at the present time.

The von Kármán analogy (eq. (1)) and the Schultz-Grunow friction formula (eq. (5)) may be combined to give the local heat-transfer coefficient in terms of the local Reynolds number:

$$St = \frac{1.60(\ln Re_x)^{-2.58}}{1 + 1.26(\ln Re_x)^{-1.29}\left[5Pr + 5\ \ln(5Pr + 1) - 14\right]} \tag{6}$$

For air, which has a Prandtl number around 0.7 (see ref. 7), equation (6) may be represented approximately in the range $10^5 < Re_x < 10^7$ by

$$StPr^{0.4} = 0.0296\ Re_x^{-0.2} \tag{7}$$

This relation is easier to use for calculations than equation (6). Comparison of equations (7) and (4) shows that, in this range,

$$StPr^{0.4} = C_f/2 \tag{8}$$

Equation (8) represents a modification of the familiar Colburn analogy (ref. 9):

$$StPr^{2/3} = C_f/2$$

The Colburn relation predicts heat-transfer coefficients for air that are too high, and the modification (eq. (8)) is better.

The foregoing equations were obtained only for constant fluid properties. If the temperature of the plate is considerably different from that of the free stream, there may be considerable variation in the fluid properties appearing in the Stanton and Reynolds numbers, and a question arises as to the best temperature for evaluation of these properties. It can be shown (ref. 10) that an adequate method for taking into consideration the influence of temperature-dependent fluid properties for gas flow in both internal and external boundary layers is to evaluate all properties at the free-stream static temperature and then to include all properties in a factor $(T_w/T_\infty)^m$, where the exponent m is a function of geometry alone. Examination of the results of reference 11 indicates that, for the turbulent incompressible boundary layer, the Stanton number varies as $(T_w/T_\infty)^{-0.4}$, other things being equal. This observation may be used to correct the foregoing equations for temperature-dependent fluid-property effects. Thus, for the simple power relation (eq. (7)) one may write

$$\mathrm{StPr}^{0.4} = 0.0296\ \mathrm{Re}_x^{-0.2}\left(\frac{T_w}{T_\infty}\right)^{-0.4} \tag{9}$$

where the Stanton number and Reynolds number are to be evaluated at the free-stream temperature.

Velocity Profiles

Data correlation. - Velocity survey data in turbulent boundary layers are usually correlated in one of three ways:

$$u/u_\infty = f_1(y/\delta) \tag{10}$$

$$u^+ = f_2(y^+) \tag{11}$$

$$u_\infty^+ - u^+ = f_3(y/\delta) \tag{12}$$

where u^+ is a dimensionless velocity, defined as

$$u^+ = \frac{u}{\sqrt{\tau_w/\rho}}$$

and y^+ is a dimensionless distance, defined as

$$y^+ = \frac{y\sqrt{\tau_w/\rho}}{\nu}$$

A plot of the type (10) may be prepared simply from measurements of the velocity in the boundary layer as a function of the distance from the wall. The methods (11) and (12) require additionally the determination of the wall shear stress τ_w. Method (10) is most satisfactory in the outer portions of the boundary layer, where the flow can be characterized by the thickness of the hydrodynamic boundary layer δ. Von Kármán (ref. 12) has given theoretical basis for the "universal velocity profile," used in the method of (11). However, it has been found experimentally that this method of correlating profiles works best near the wall, where free-stream conditions have the least influence. The third type of plot (12), which is often referred to as the "universal velocity deficiency law," represents attempts to tie the wall effects to the free-stream effects by introducing both the wall shear stress and the boundary-layer thickness. Data plotted on this basis correlate nicely in the outer regions of the boundary layer ($y/\delta > 0.01$), but the method fails near the wall.

The boundary-layer "thickness" is a rather nebulous thing, since in reality the boundary-layer velocity reaches the free-stream velocity at an infinite distance from the plate. However, the velocity is almost equal to the free-stream velocity a short distance from the plate; and it is this distance that is usually referred to as the "boundary-layer thickness." There then arises a question as to how much is "almost," or, in other words, what fraction of the free-stream velocity occurs at the "edge" of the boundary layer. Often the distance at which the velocity is 99 percent of the free-stream velocity is taken as the boundary-layer thickness; however, this definition has no physical meaning and moreover is difficult to determine accurately from experimental data. In integral treatments of the boundary layer, some relation of the type (10) would be advantageous, where a "boundary-layer thickness" is used to characterize velocity profile in the boundary layer. Therefore, some means is desired of evaluating for experimental surveys the same boundary-layer thickness used in the integral methods. A meaningful boundary-layer thickness can be determined by making use of the fact that turbulent velocity profiles can, to a good approximation, be represented by equations of the form

$$\frac{u}{u_\infty} = \left(\frac{y}{\delta}\right)^{1/m} \tag{13}$$

The power parameter m is about 5 to 8. For a profile of this type, the boundary-layer thickness δ is related to the displacement thickness δ^*, which has real physical meaning, by

$$\delta = (1 + m)\delta^* \tag{14}$$

The displacement thickness δ^* can be determined quite accurately by integration of the velocity profile; m can be determined by plotting

u/u_∞ against y on log-log paper. Then, δ may be calculated from equation (14). This technique allows calculation of a meaningful δ that corresponds to the δ used in integral analyses. This method has been used in the reduction of velocity survey data obtained in this investigation; the values of δ calculated in this manner are quite close to the values of the "99-percent" boundary-layer thickness.

Universal velocity profile for flat plate. - A velocity profile of the type (11) is well known for fully established turbulent flow in a pipe; this is the familiar universal velocity profile for turbulent flow in pipes, which is based largely on the experimental data of Nikuradse (ref. 8). The velocity profile in an external turbulent boundary layer is not expected to be too different from that found in a pipe, and this assumption has been used by numerous investigators in analyzing turbulent boundary layers (ref. 5). The main differences between internal and external shear flows occur away from the wall, where the free-stream conditions may influence the boundary layer. However, the two flows should be quite similar near the wall, where the wall effects predominate. A great deal of accurate flat-plate velocity-profile data has been obtained by Schultz-Grunow (ref. 6), who also made wall shear-stress measurements. However, these data are limited to the outer regions of the turbulent boundary layer, and no data were obtained in the laminar sublayer region. However, by combination of the Schultz-Grunow flat-plate survey data and the universal velocity profile for pipe flow, a suitable universal velocity profile can be constructed for a flat plate. This has been done here, and the details of this combination are presented in the following paragraphs.

The boundary layer has been divided into four distinct regions:

(1) A laminar sublayer formed near the wall

(2) A buffer region adjacent to the laminar sublayer

(3) A turbulent core adjacent to the buffer layer and extending over about 1/3 of the boundary layer

(4) A turbulent wake, which extends from the core to the free stream, approximately 2/3 of the boundary layer

In the laminar sublayer, the mechanism for momentum diffusion is entirely viscous, so that

$$\tau_{bl} = \mu \frac{\partial u}{\partial y}$$

Because this sublayer is so thin, the shear stress is essentially constant and equal to its value at the wall τ_w. Thus, by suitable

manipulations and integration, the preceding relation leads to the equation for the velocity in the sublayer:

$$u^+ = y^+ \tag{15}$$

Very little data have been obtained in the laminar sublayer; therefore it is difficult to tell how far from the wall it extends. It is common to assume that, in a pipe, the sublayer extends to $y^+ = 5$, and it is assumed that this value is reasonable for the external boundary layer as well.

The buffer layer is the region near the wall where momentum diffusion by turbulent eddies becomes more important. Velocity surveys in pipes indicate that the buffer layer may be described by (ref. 5)

$$u^+ = -3.05 + 5.0 \ln y^+ \tag{16}$$

The extent of the buffer layer can be examined by plotting u^+ against y^+ on semilogarithmic paper, which renders (16) a straight line (see fig. 1). At the outer edge of the buffer layer, a distinct break is observed, and in the pipe-flow data this break occurs at about $y^+ = 30$. Upon examination of these data, von Kármán took $y^+ = 30$ as the outer edge of the pipe-flow buffer layer (ref. 5). The data of Schultz-Grunow do not extend below $y^+ = 50$ (ref. 6), but an extrapolation of his data towards the wall intersects the pipe-flow buffer layer (eq. (16)) at about $y^+ = 18.2$. It therefore seems reasonable to give this value as the outer edge of the buffer layer for the flat-plate turbulent boundary layer.

The velocity profile in the turbulent core of the flat-plate boundary layer is obtained entirely from Schultz-Grunow's data, which indicate that, in the core,

$$u^+ = 4.4 + 2.43 \ln y^+ \tag{17}$$

Figure 1 indicates that the core extends from y^+ of 18.2 to 360.

In the region of the turbulent wake, for y^+ greater than 360, Schultz-Grunow's data exhibit considerable scatter, and the best interpretation of the data in this region appears to be

$$u^+ = -4.4 + 3.96 \ln y^+ \tag{18}$$

Because of the influence of free-stream conditions, the velocity data do not correlate as well in the turbulent wake as in the inner regions, as both the data of Schultz-Grunow and the present data show (fig. 1).

To summarize, a universal velocity profile for the flat plate has been obtained by "patching" the boundary-layer data of Schultz-Grunow to the familiar universal velocity profile found for turbulent flow in pipes. This results in a four-region boundary layer as follows:

(1) Laminar sublayer (eq. (15)): $0 < y^+ < 5$

(2) Buffer layer (eq. (16)): $5 < y^+ < 18.2$

(3) Turbulent core (eq. (17)): $18.2 < y^+ < 360$

(4) Turbulent wake (eq. (18)): $y^+ > 360$

Temperature Profiles

Similarity of velocity and temperature fields. - Because of the similarity between the mechanisms of heat and momentum transfer, the temperature field in a boundary layer can be examined by consideration of the velocity profile. This is especially true for a flat plate at constant temperature, as can be seen by examination of the differential equations and boundary conditions for heat and momentum transfer. The momentum equation for the turbulent incompressible boundary layer on a flat plate may be written as

$$\frac{u}{u_\infty}\frac{\partial(u/u_\infty)}{\partial x} + \frac{v}{u_\infty}\frac{\partial(u/u_\infty)}{\partial y} = \frac{1}{u_\infty}\frac{\partial}{\partial y}\left[(\nu + \epsilon_M)\frac{\partial(u/u_\infty)}{\partial y}\right] \tag{19a}$$

where the shear stress in the boundary layer is given by

$$\frac{\tau_{bl}}{\rho} = (\nu + \epsilon_M)\frac{\partial u(x,y)}{\partial y} \tag{19b}$$

Equation (19a) is subject to the boundary conditions

$$\frac{u(x,0)}{u_\infty} = 0 \qquad \frac{u(x,\infty)}{u_\infty} = 1$$

Similarly, the energy equation of the turbulent incompressible boundary layer may be written as (for constant wall temperature, dissipation terms neglected)

$$\frac{u}{u_\infty}\frac{\partial\theta}{\partial x} + \frac{v}{u_\infty}\frac{\partial\theta}{\partial y} = \frac{1}{u_\infty}\frac{\partial}{\partial y}\left[\left(\frac{\nu}{Pr} + \epsilon_H\right)\frac{\partial\theta}{\partial y}\right] \tag{20a}$$

where the heat flux in the boundary layer is

$$\frac{q''_{bl}}{\rho c_p} = -(\alpha + \epsilon_H) \frac{\partial t_{bl}}{\partial y} \tag{20b}$$

The dimensionless temperature θ is defined by

$$\theta = \frac{t_w - t_{bl}}{t_w - t_\infty} = \theta(x,y) .$$

The energy equation is subject to the boundary conditions

$$\theta(x,0) = 0 \qquad \theta(x,\infty) = 1$$

The quantities ϵ_M and ϵ_H are defined as the eddy diffusivities for momentum and heat, respectively, and it is well known that the ratio ϵ_H/ϵ_M is near unity for gases and other fluids with Prandtl numbers near 1. If the Prandtl number is 1, and if the eddy diffusivities are equal, the momentum and energy equations of the boundary layer are identical in form. Moreover, since the plate is at constant temperature, their boundary conditions are identical. Therefore, the solutions of the two equations must be the same, and the velocity profile u/u_∞ is equal to the dimensionless-temperature profile θ.

If the fluid has a Prandtl number near unity, and the diffusivities are approximately equal, the temperature and velocity profiles would be expected to be quite similar in shape. It is generally observed that, for the turbulent boundary layer of air on a flat plate at constant temperature, the velocity and temperature profiles are similar when based on their own boundary-layer thicknesses. In other words, experiments indicate that

$$\frac{u}{u_\infty} = f\left(\frac{y}{\delta}\right) \qquad \theta = f\left(\frac{y}{\delta_T}\right)$$

where δ and δ_T are the thicknesses of the hydrodynamic and thermal boundary layers, respectively. This similarity is of great importance in integral treatments of turbulent heat transfer. Rubesin (ref. 13) shows that, for constant wall temperature, the hydrodynamic and thermal boundary layers are related by

$$\frac{\delta_T}{\delta} = Pr^{-7/12}$$

Thus, for air, having a Prandtl number of 0.7, the thermal boundary layer is about 23 percent thicker than the hydrodynamic boundary layer. It is important to emphasize that similarity is obtained only when the profiles are characterized by their own boundary-layer thicknesses.

Universal temperature profile. - An alternative method of determining the temperature profile in the turbulent boundary layer for fluids with Prandtl numbers different from unity is to use the analogy between heat and momentum transfer. This idea was first suggested by von Kármán (ref. 5). A dimensionless temperature t^+ may be defined as

$$t^+ = (t_w - t_{bl})\rho c_p \sqrt{\tau_w/\rho}/q''_w$$

By dimensional analysis, one may reason that t^+, like u^+, should be a function of y^+ only (see ref. 12). Under this assumption, equations (19b) and (20b), respectively, may be written as

$$\frac{\tau_{bl}}{\tau_w} = \left(1 + \frac{\epsilon_M}{\nu}\right)\frac{du^+}{dy^+} \tag{21}$$

and

$$\frac{q''_{bl}}{q''_w} = \left(\frac{1}{Pr} + \frac{\epsilon_H}{\nu}\right)\frac{dt^+}{dy^+} \tag{22}$$

If one has on hand a suitable universal velocity profile (u^+ against y^+), postulates the Reynolds analogy ($\epsilon_H = \epsilon_M$), and makes some assumptions about the shear-stress and heat-flux distribution in the boundary layer, he may compute from equations (21) and (22) the universal temperature profile, t^+ against y^+. This will now be done for the flat-plate profile discussed previously.

In the laminar sublayer, heat and momentum transfers are due entirely to molecular transports, and turbulent transfers are unimportant. Thus, the eddy diffusivities for heat and momentum are both zero. Moreover, the sublayer is so thin that the shear stress and heat flux are essentially constant through the layer. Thus, by dividing equation (22) by (21) and noting from (15) that $u^+ = y^+$, the following is obtained:

$$dt^+ = Pr\ dy^+$$

which may be integrated to give the temperature distribution in the sublayer (since $t^+ = 0$ when $y^+ = 0$),

$$t^+ = Pr\ y^+ \qquad 0 < y^+ < 5 \tag{23}$$

In the buffer layer, the shear stress and heat flux are again assumed to be constant. However, turbulent heat and momentum transfer begins to be important in this layer, so that both molecular and turbulent effects must be considered. The eddy diffusivity for momentum may be determined by substituting the velocity profile (eq. (16)) into (21) and integrating from $y^+ = 5$, where $u^+ = 5$:

$$\frac{\epsilon_M}{\nu} = \frac{y^+}{5} - 1 \tag{24}$$

Now postulating the Reynolds analogy, that $\epsilon_H = \epsilon_M$, equation (22) may be integrated from $y^+ = 5$, where $t^+ = 5\ Pr$, to obtain

$$t^+ = 5Pr + 5\ \ln\left(Pr\ \frac{y^+}{5} + 1 - Pr\right) \qquad 5 < y^+ < 18.2 \tag{25}$$

In the turbulent core the laminar terms are negligible, as practically all heat and momentum are transferred by turbulent eddies. If it is assumed that the shear stress and heat flux vary in the same manner in the outer regions of the boundary layer, then division of equation (22) by equation (21) gives

$$dt^+ = du^+ \tag{26}$$

Integrating this relation from $y^+ = 18.2$, where $t^+ = 5Pr + 5\ \ln(2.65Pr + 1)$, and $u^+ = 11.45$, and substiting the velocity profile (17) result in

$$t^+ = 5Pr - 7.05 + 5\ \ln(2.64\ Pr + 1) + 2.43\ \ln\ y^+ \qquad 18.2 < y^+ < 360 \tag{27}$$

In the turbulent wake, the laminar terms are again neglected, and it is assumed that the shear stress and heat flux vary in the same manner. Then, using equation (26) and the velocity profile equation (18),

$$t^+ = 5Pr - 16.1 + 5\ \ln(2.64\ Pr + 1) + 3.96\ \ln\ y^+ \qquad 360 < y^+ < \delta_T^+ \tag{28}$$

Naturally, equation (28) is valid only inside the thermal boundary layer, where y^+ is less than $\delta_T^+ = \delta_T\sqrt{\tau_w/\rho}/\nu$.

It should be emphasized that the universal temperature profile derived applies only to a flat plate at constant temperature. Only in this case are the differential equations and boundary conditions for heat and momentum transfer similar in form, which makes the assumption that the shear stress and heat flux vary in the same manner reasonable. Figure 2 shows the predicted temperature profile compared with some experiments of the present investigation.

EXPERIMENTAL APPARATUS AND PROCEDURE

Apparatus

The plate used in this investigation had an active flow length of 60.5 inches and was tested in the 7.5-foot-diameter free-jet wind tunnel

at the Guggenheim Aeronautical Laboratory of Stanford University. Reynolds numbers up to 3.5×10^6 could be obtained with air velocities up to 130 feet per second.

The active surface was built up of 24 individually heated copper strips, which were thermally insulated from each other. The surface was varnished and rubbed down several times to give a hydraulically smooth surface. The inactive side of the plate was well insulated so that the "back leak" was minimized. Heat meters were installed at several places on both the inactive side and at the ends of the heated strips so that the back leak and "end leak" could be measured accurately. The emissivity of the heated surface was measured in order that radiation from this surface could be determined. The insulation between the various strips provided a "heat meter," so that conduction between strips could be estimated.

Iron-constantan thermocouples were located near the surface at the center of each strip and at several other points in the strip. The thermocouples were referenced to a small copper plate mounted on one side of the heated surface; the reference plate in turn was referenced to distilled-water ice at 32° F. This arrangement provided for a direct measurement of the temperature difference. Pressure taps located at several points on the active surface allowed measurement of static pressure on the flat plate. A wattmeter was used to determine the power dissipated by each heater. The plate construction is described in detail in reference 14 and is considered at greater length in appendix A of reference 1.

Because of the end leak and because the heaters did not extend the full width of the strips, the center temperature was somewhat higher than the average temperature. The mean temperature was analyzed in terms of the center temperature, which allows correction of the center temperatures to obtain the correct mean temperature differences. The analysis was verified by measurement of the transverse temperature distribution, which was then integrated to give the mean temperature; good agreement with the analysis was obtained, the correction being about 13 percent. The analysis of transverse temperature distribution is described in appendix B of reference 1.

The plate is shown before installation in the wind tunnel in figure 3(a). The dimensions of the active side are given in figure 3(b). The heated strips are wider nearer the front in order to minimize contamination of the hot boundary layer by sidewise mixing with the cold boundary layers on the unheated portions.

Figures 4(a) and (b) show the plate installed in the wind tunnel. The thermocouple, power, and pressure leads can be seen coming from the sides of the plate. In order to facilitate handling of probes near the

active surface, a traversing mechanism was constructed. This mechanism (fig. 4(c)) consisted of a streamlined beam suspended on tracks beneath the plate. The probes were rigidly supported by a micrometer arrangement well in front of the beam and could be moved normal to the surface or in the flow direction.

The free-stream velocity was measured with a Pitot-static tube. Velocity surveys in the boundary layer were made with a specially constructed Pitot tube made of a hyperdermic tube having an outside diameter of 0.020 inch and an inner diameter of 0.010 inch. Temperature surveys were made with a specially constructed thermocouple consisting of a butt-welded iron-constantan thermocouple flattened to a thickness of 0.002 inch and supported by heavier iron and constantan wires. The thermocouple probe was referenced directly to the free-stream temperature. This probe is shown in figure 5.

Data-Recording Procedure

To make a test run, the power to each strip was adjusted to give the desired wall-temperature distribution. After steady-state conditions were obtained, the center temperature and the power to each strip were measured. The free-stream velocity over each strip was then measured with a Pitot-static tube that was positioned by the traversing mechanism. Other necessary measurements were the readings of the various heat meters, the temperature of the thermocouple reference plate, and wet and dry bulb temperatures. These measurements allowed determination of the local Stanton and Reynolds numbers.

Transition from laminar to turbulent flow, which was stimulated by a strip of cellophane tape, occurred in each case on the first strip, as was indicated by the nature of the heat-transfer measurements.

Data Reduction

The heat leak from the back side of the plate and from the ends of each strip was evaluated from the heat-meter readings. The radiation heat transfer from the front of the plate was calculated from the temperature at the center of the strip, and the conduction between strips was calculated from the center temperatures and an estimated value of the thermal resistance between strips. A first approximation to the convective heat transfer was then found by subtracting the various heat leaks from the measured power input. A first approximation to the heat-transfer coefficient was obtained by dividing the approximate convection heat transfer by the temperature difference at the center of the strip. This allowed estimation of the ratio of the mean temperature difference to the

center temperature difference from the analysis of transverse temperature distribution. Using the estimated mean temperature difference, second approximations to the radiation (based on the mean temperature), the heat transfer, and the conductance were calculated; then a new estimate of the mean temperature correction was made, again using the analysis. This iterative process was repeated until the heat-transfer rate, the mean temperature difference, and the heat-transfer coefficient were all in agreement. Usually only one iteration was required.

Reduction of dynamic-pressure measurements in the usual manner led to calculation of the mass velocity. A humidity correction was made in determining the air density. The local Stanton and Reynolds numbers were then calculated, basing all fluid properties on the free-stream temperature. The temperature-dependent fluid-properties correction, $(T_w/T_\infty)^{0.4}$, was evaluated with the mean temperature of the strip, and the corrections on the Stanton numbers were of the order of 2 percent.

Pressure Distribution and Free-Stream Turbulence Level

After installing the plate in the wind tunnel, the angle of attack of the plate was adjusted to give the best possible pressure distribution on the heated surface. The final pressure distribution (fig. 6) is considered satisfactory.

The free-stream turbulence level was measured by hot-wire-anemometry techniques. The equipment used in these measurements is described in reference 15, and the results are shown by figure 7. The turbulence level was higher near the front of the plate and increased with increasing velocity. The turbulence intensity over most of the plate during typical runs was of the order of 2 to 3 percent.

Precision

An analysis of the experimental uncertainty indicated that the probable error in the local Stanton numbers is ± 3 percent, and the probable error in the local Reynolds number is ± 1 percent. These values agree with the standard deviation of the experimental Stanton numbers from the isothermal equation (9), which was calculated as 4.5 percent. The analysis of experimental uncertainty is presented in detail in appendix A of reference 1.

RESULTS AND DISCUSSION

Heat-Transfer Data

Eight isothermal heat-transfer runs were made at velocities ranging from 43 to 127 feet per second. Figure 8 shows the results of these tests, the data of which are tabulated in table I(a). The measured local Stanton numbers, corrected for fluid-property variations by the factor $(T_w/T_\infty)^{0.4}$, are plotted against the local Reynolds numbers, based on the free-stream temperature. The data are compared with the von Kármán analogy, employing the Schultz-Grunow friction factor (eq. (6)) and the simple power equation (9). The data are in good agreement with these relations over the Reynolds number range $10^5 < Re_x < 3.5 \times 10^6$. The standard deviation of the experimental Stanton numbers from the power formula is 4.5 percent.

Velocity Survey Data

Velocity surveys were taken at three points on the plate and at two different free-stream velocities. The purpose of these surveys was to demonstrate that the profiles were in agreement with the standard boundary-layer profiles and that thus there were no flow anomalies. These data are compared with the universal velocity profile for a flat plate (eqs. (15) to (18)) in figure 1. In reducing the survey data to a u^+ against y^+ basis, the wall shear stress was computed from the Schultz-Grunow expression for the friction factor (eq. (5)). The agreement of these data with the universal profile is quite good, except in the turbulent wake region where the correlation is not expected to be as satisfactory. The data are compared with the universal velocity deficiency profile of Schultz-Grunow in figure 9. Since the Schultz-Grunow friction-factor relation (5) was obtained from this deficiency profile, and since the data based on wall shear values from equation (5) agree quite well with the deficiency profile, it is felt that equation (5) is entirely adequate for determining the friction factors for the apparatus of the present investigation.

The data are compared with the power profiles in figure 10, which shows that, in this Reynolds number range, the 1/5.6-power profile

$$\frac{u}{u_\infty} = \left(\frac{y}{\delta}\right)^{1/5.6} \tag{29}$$

is the best fit of the data. The 1/7-power profile does not agree well in this Reynolds number range. The Schultz-Grunow velocity profile for

a Reynolds number of 10^6 is in good agreement with the data and with the 1/5.6-power profile. The velocity survey data are tabulated in table I(b).

In reducing the velocity survey data, the hydrodynamic boundary-layer thickness δ was determined by the method described earlier. The dimensionless velocity u/u_∞ was plotted against the distance from the wall on log-log paper, and the best "power formula fit" was obtained. The profile was then integrated to obtain the displacement thickness δ^*, which can be related to δ. The boundary-layer thickness determined in this manner is the same one that is used in integral analysis; this thickness is approximately the same as the 99-percent thickness (the y for which $u/u_\infty = 0.99$).

Temperature Survey Data

Temperature surveys in the boundary layer were made at three points on the plate for two different free-stream velocities (table I(c)). A typical profile is shown in figure 11. The purpose of these surveys was to obtain profiles for constant wall temperature that would serve as a basis of comparison for the profiles taken with a step wall-temperature distribution (ref. 2). As a matter of general interest, these data are also compared with the universal temperature profile predicted from the universal velocity profile. Because of the uncertainty in location of the thermocouple probe, it was necessary to "shift" the data so that the temperatures extrapolated to the wall value with the correct slope. The temperature gradient at the wall was determined from equation (9) and the Fourier heat-conduction equation

$$q''_{bl} = -k \frac{\partial t_{bl}}{\partial y}$$

which applies, since the flow near the wall is laminar. Both positive and negative shifts were necessary, indicating that the error was of a random nature. The method of the shift is indicated by figure 11. In no case did the shift exceed 0.002 inch, the average shift being about 0.001 inch.

The temperature survey data are compared with the universal temperature profile predicted earlier from the velocity profile in figure 2. In reducing the survey data to a t^+ against y^+ form, the wall shear stress was determined from the Schultz-Grunow friction factor (eq. (5)), and the wall heat flux was determined from the power relation (eq. (9)). The data agree well with the predicted profile in the laminar sublayer and in the buffer layer, but in the turbulent core the agreement is not too good. This is probably due to the fact that the eddy diffusivities

for heat and momentum are not equal in the turbulent core, as was assumed in the profile prediction. In fact, it is expected that the largest departure from this assumption occurs in the core. Reference 16 proposes an analysis from which the ratio of eddy diffusivities may be determined as a function of the Prandtl number and the quantity ϵ_M/ν. This analysis indicates that the ratio ϵ_H/ϵ_M is unity when $Pr = 1$ and $\epsilon_M/\nu = 1$, but that $\epsilon_H/\epsilon_M > 1$ when $\epsilon_M/\nu > 1$. Moreover, the departure from equal diffusivities is greatest when the turbulent portion of the momentum transfer is greatest, and this point occurs somewhere in the turbulent core. For air, the ratio of diffusivities is about 1.1 to 1.3. This explains why the data do not agree well with the predicted temperatures in this region.

Although the temperature and velocity profiles are not too "similar" when considered on a t^+ and u^+ against y^+ basis, the profiles do have similar shapes when the distances from the wall are characterized by the thicknesses of the respective hydrodynamic and thermal boundary layers. The velocity profiles were found to follow the 1/5.6-power formula,

$$\frac{u}{u_\infty} = \left(\frac{y}{\delta}\right)^{1/5.6} \tag{29}$$

The temperature profiles can be represented by a similar relation, where the thermal boundary-layer thickness δ_T is employed:

$$\theta = \left(\frac{y}{\delta_T}\right)^{1/5.6} \tag{30}$$

The temperature survey data are compared with power formulas in figure 12. The 1/5.6-power curve is the best fit, indicating that the velocity and temperature profiles are indeed similar when each is referred to its respective boundary-layer thickness. This empirical observation is of considerable importance in integral analyses of turbulent-boundary-layer heat transfer.

In reducing the temperature survey data, the thermal boundary-layer thickness δ_T was determined by the same method employed in evaluating the hydrodynamic boundary-layer thickness δ. The dimensionless temperature θ was plotted against the distance from the wall on log-log paper, and the "best power" behavior was determined. In each case it was found that θ varied almost as the distance from the wall to the 1/5.6 power. The conduction thickness δ_T^* was then determined by numerical integration of the temperature profile; δ_T^* is related to δ_T for power profiles by

$$\delta_T = (1 + m)\delta_T^* \tag{31}$$

if $\theta = (y/\delta_T)^{1/m}$. This technique allowed determination of the same δ_T that is used in integral analyses; the thicknesses determined in this manner were approximately the same as the 99-percent thicknesses (the y for which $\theta = 0.99$).

SUMMARY OF RESULTS

The heat-transfer data for an isothermal plate are in good agreement with the best available analyses over the Reynolds number range $10^5 < Re_x < 3.5 \times 10^6$. For air, a satisfactory power representation of the more complicated von Kármán analogy is

$$StPr^{0.4} = 0.0296\, Re_x^{-0.2} \left(\frac{T_w}{T_\infty}\right)^{-0.4} \tag{9}$$

The Stanton, Prandtl, and Reynolds numbers in this relation are to be evaluated at the free-stream temperature.

The velocity profiles agree well with the well-known profiles of Schultz-Grunow, and, in the Reynolds number range of the tests, the data may be represented by a power formula

$$\frac{u}{u_\infty} = \left(\frac{y}{\delta}\right)^{1/5.6} \tag{29}$$

The temperature profiles are similar to the velocity profiles if each is characterized by its respective boundary-layer thickness. The temperature profile in the Reynolds number range of the tests can be represented by

$$\theta = \left(\frac{y}{\delta_T}\right)^{1/5.6} \tag{30}$$

Stanford University,
Stanford, Calif., October 22, 1957.

REFERENCES

1. Reynolds, W. C.: Heat Transfer in the Turbulent Incompressible Boundary Layer with Constant and Variable Wall Temperature. Ph.D. Thesis, Stanford Univ., 1957.

2. Reynolds, W. C., Kays, W. M., and Kline, S. J.: Heat Transfer in the Turbulent Incompressible Boundary Layer. II - Step Wall-Temperature Distribution. NASA MEMO 12-2-58W, 1958.

3. Reynolds, W. C., Kays, W. M., and Kline, S. J.: Heat Transfer in the Turbulent Incompressible Boundary Layer. III - Arbitrary Wall Temperature and Heat Flux. NASA MEMO 12-3-58W, 1958.

4. Reynolds, W. C., Kays, W. M., and Kline, S. J.: Heat Transfer in the Turbulent Incompressible Boundary Layer. IV - Effect of Location of Transition and Prediction of Heat Transfer in a Known Transition Region. NASA MEMO 12-4-58W, 1958.

5. von Kármán, Th.: The Analogy Between Fluid Friction and Heat Transfer. ASME Trans., vol. 61, no. 8, Nov. 1939, pp. 705-710.

6. Schultz-Grunow, F.: New Frictional Resistance Law for Smooth Plates. NACA TM 986, 1941.

7. Keenan, Joseph H., and Kaye, Joseph: Gas Tables. John Wiley & Sons, Inc., 1948.

8. Nikuradse, J.: Gesetzmässigkeiten der Turbulenten Strömung in Glatten Rohren. Forsch. Geb. Ing.-Wes., Bd. 3, ed. B, Sept.-Oct. 1932.

9. Colburn, Allan P.: A Method of Correlating Forced Convection Heat Transfer Data and a Comparison with Fluid Friction. Trans. Am. Inst. Chem. Eng., vol. XXIX, 1933, pp. 174-206.

10. Kays, W. M.: A Summary of Experiments and Analysis for Gas Flow Heat Transfer and Friction in Circular Tubes. TR-22, Dept. Mech. Eng., Stanford Univ., June 30, 1954. (Contract N6onr-251.)

11. Deissler, R. G., and Loeffler, A. L.: Turbulent Flow and Heat Transfer on a Flat Plate at High Mach Number with Variable Fluid Properties. ASME Paper No. 55-A-133, 1955.

12. Schlichting, Hermann: Boundary Layer Theory. McGraw-Hill Book Co., Inc., 1955, p. 392.

13. Rubesin, Morris W.: The Effect of an Arbitrary Surface-Temperature Variation Along a Flat Plate on the Convective Heat Transfer in an Incompressible Turbulent Boundary Layer. NACA TN 2345, 1951.

14. Satterlee, H. M.: An Experimental Investigation of Heat Transfer in the Turbulent Boundary Layer on a Flat Plate: Design of Apparatus. Eng. Thesis, Stanford Univ., 1955.

15. Anon.: Hot Wire Anemometry Equipment Specifications. The Flow Corp., Cambridge (Mass.).

16. Jenkins, Rodman: Variation of the Eddy Conductivity with Prandtl Modulus and Its Use in Prediction of Turbulent Heat Transfer Coefficients. Preprints of papers for Heat Transfer and Fluid Mech. Inst. pub. by Stanford Univ. Press, 1951, pp. 147-158.

TABLE I. - EXPERIMENTAL DATA SUMMARY

(a) Heat-transfer data

Strip	G, $\frac{lb}{(hr)(sq\ ft)} \times 10^{-3}$	Δt_m, ^oF	q''_w, $\frac{Btu}{(hr)(sq\ ft)}$	h, $\frac{Btu}{(hr)(sq\ ft)(^oF)}$	St $\times 10^3$	$St\left(\frac{T_w}{T_\infty}\right)^{0.4} \times 10^3$	$Re_x \times 10^{-6}$	G, $\frac{lb}{(hr)(sq\ ft)} \times 10^{-3}$	Δt_m, ^oF	q''_w, $\frac{Btu}{(hr)(sq\ ft)}$	h, $\frac{Btu}{(hr)(sq\ ft)(^oF)}$	St $\times 10^3$	$St\left(\frac{T_w}{T_\infty}\right)^{0.4} \times 10^3$	$Re_x \times 10^{-6}$
	Nominal u_∞ = 127 ft/sec; t_∞ = 86.1° F; ρ_∞ = 0.0729 lb/cu ft							Nominal u_∞ = 120 ft/sec; t_∞ = 73.9° F; ρ_∞ = 0.0746 lb/cu ft						
2	33.3	22.2	483	21.7	2.73	2.77	0.255	32.0	22.8	467	20.5	2.67	2.72	0.249
3	33.7	22.7	442	19.4	2.41	2.45	.423	32.1	23.1	431	18.7	2.42	2.46	.410
4	33.7	22.4	386	17.2	2.13	2.17	.580	32.1	22.9	382	16.7	2.17	2.20	.562
5	33.7	22.5	384	17.1	2.11	2.15	.736	32.1	23.2	381	16.4	2.14	2.17	.712
6	33.6	22.5	375	16.7	2.06	2.10	.889	32.1	23.0	369	16.0	2.08	2.16	.865
7	33.6	22.6	367	16.3	2.02	2.06	1.045	32.2	23.3	367	15.8	2.04	2.08	1.020
8	33.5	22.6	358	15.8	1.97	2.00	1.196	32.2	23.3	356	15.3	1.98	2.01	1.172
9	33.5	22.9	370	16.2	2.01	2.05	1.353	32.2	23.3	360	15.5	1.99	2.03	1.325
10	33.4	23.0	339	14.7	1.85	1.88	1.507	32.2	23.3	328	14.0	1.81	1.84	1.484
11	33.5	23.1	332	14.3	1.79	1.82	1.661	32.2	23.6	323	13.7	1.77	1.80	1.630
12	33.6	23.0	341	14.8	1.84	1.87	1.823	32.3	23.5	336	14.3	1.85	1.88	1.788
13	33.4	22.8	326	14.3	1.78	1.82	1.970	32.2	23.4	323	13.8	1.78	1.81	1.863
14	33.5	22.6	325	14.3	1.79	1.82	2.13	32.2	23.4	325	13.9	1.80	1.83	2.09
15	33.4	22.9	317	13.8	1.73	1.76	2.28	32.1	23.9	321	13.4	1.74	1.77	2.23
16	33.4	22.9	320	13.9	1.74	1.77	2.44	32.2	23.9	326	13.6	1.76	1.79	2.39
17	33.5	23.1	325	14.0	1.75	1.78	2.60	32.3	23.6	320	13.6	1.75	1.78	2.55
18	33.5	23.1	317	13.8	1.72	1.75	2.75	32.2	24.0	315	13.1	1.70	1.73	2.70
19	33.5	23.3	314	13.5	1.68	1.71	2.90	32.1	24.0	316	13.1	1.69	1.72	2.84
20	33.4	23.3	322	13.8	1.73	1.76	3.05	32.1	24.2	318	13.2	1.71	1.74	2.99
21	33.2	23.2	308	13.3	1.67	1.70	3.18	32.1	24.1	303	12.6	1.64	1.66	3.14
22	33.3	23.5	289	12.3	1.54	1.59	3.36	32.1	24.5	287	11.7	1.52	1.55	3.30
23	33.3	23.6	299	12.7	1.58	1.61	3.51	32.1	24.5	298	12.2	1.58	1.60	3.45
	Nominal u_∞ = 113 ft/sec; t_∞ = 74.7° F; ρ_∞ = 0.0746 lb/cu ft							Nominal u_∞ = 109 ft/sec; t_∞ = 74.9° F; ρ_∞ = 0.0745 lb/cu ft						
2	30.2	23.4	434	18.6	2.56	2.60	0.235	28.9	23.2	387	16.7	2.41	2.45	0.225
3	30.3	23.2	418	18.0	2.48	2.53	.386	29.2	23.1	405	17.5	2.51	2.55	.372
4	30.3	23.1	375	16.2	2.23	2.27	.528	29.0	23.0	362	15.7	2.26	2.30	.507
5	30.5	23.4	365	15.6	2.13	2.17	.676	29.2	23.5	359	15.3	2.18	2.22	.648
6	30.4	23.3	361	15.5	2.12	2.16	.816	29.3	23.3	348	14.9	2.13	2.16	.788
7	30.4	23.6	359	14.8	2.05	2.07	.960	29.3	23.6	347	14.7	2.10	2.13	.924
8	30.5	23.6	347	14.7	2.01	2.05	1.108	29.3	23.7	335	14.1	2.01	2.05	1.064
9	30.4	23.6	352	14.9	2.05	2.09	1.247	29.3	23.5	341	14.5	2.07	2.10	1.203
10	30.5	23.6	319	13.5	1.84	1.88	1.398	29.4	23.7	309	13.0	1.85	1.88	1.344
11	30.5	23.9	315	14.3	1.95	1.99	1.539	29.4	23.9	306	12.8	1.81	1.85	1.481
12	30.5	24.0	325	13.5	1.85	1.88	1.682	29.3	24.0	318	13.2	1.89	1.92	1.613
13	30.5	23.7	317	13.4	1.83	1.86	1.828	29.4	23.8	306	12.9	1.83	1.86	1.759
14	30.6	23.9	318	13.3	1.81	1.84	1.978	29.3	23.8	309	12.9	1.85	1.88	1.891
15	30.4	24.3	313	12.9	1.77	1.80	2.11	29.3	24.4	303	12.4	1.77	1.80	2.03
16	30.4	24.4	316	13.0	1.78	1.81	2.25	29.3	24.4	309	12.6	1.80	1.83	2.17
17	30.4	24.3	310	12.7	1.74	1.77	2.40	29.1	24.3	305	12.5	1.79	1.82	2.29
18	30.4	24.5	307	12.5	1.72	1.75	2.54	29.3	24.6	296	12.0	1.71	1.77	2.45
19	30.4	24.6	306	12.4	1.71	1.74	2.68	29.3	24.6	291	11.8	1.69	1.72	2.58
20	30.3	24.7	309	12.5	1.72	1.75	2.80	29.0	24.7	298	12.1	1.74	1.77	2.69
21	30.3	24.5	295	12.0	1.66	1.69	2.95	29.0	24.5	285	11.6	1.67	1.70	2.83
22	30.3	24.7	275	11.1	1.53	1.56	3.10	29.1	24.7	267	10.8	1.54	1.57	2.98
23	30.3	24.8	285	11.5	1.58	1.61	3.25	29.1	24.8	275	11.1	1.59	1.62	3.12
	Nominal u_∞ = 99 ft/sec; t_∞ = 66.3° F; ρ_∞ = 0.0757 lb/cu ft							Nominal u_∞ = 83 ft/sec; t_∞ = 71.0° F; ρ_∞ = 0.0760 lb/cu ft						
2	26.8	21.2	392	18.5	2.87	2.92	0.211	22.6	20.0	328	16.37	3.02	3.06	0.177
3	26.9	21.1	342	16.2	2.51	2.55	.347	22.6	20.3	284	13.99	2.59	2.62	.289
4	26.9	21.5	307	14.3	2.21	2.25	.475	22.6	20.4	248	12.17	2.25	2.28	.396
5	26.8	21.5	299	13.9	2.15	2.19	.603	22.7	20.4	255	12.52	2.30	2.33	.506
6	27.0	21.3	290	13.6	2.11	2.14	.733	22.6	20.5	249	12.11	2.23	2.27	.611
7	27.0	21.4	290	13.6	2.10	2.13	.862	22.7	20.5	243	11.84	2.18	2.21	.721
8	26.9	21.4	275	12.9	1.99	2.02	.988	22.7	20.5	233	11.37	2.09	2.12	.829
9	26.9	21.5	284	13.2	2.05	2.09	1.115	22.7	20.5	237	11.54	2.11	2.14	.938
10	27.0	21.6	261	12.1	1.87	1.90	1.250	22.7	20.7	224	10.84	1.99	2.01	1.047
11	26.9	21.7	253	11.7	1.81	1.84	1.373	22.7	21.1	220	10.44	1.91	1.94	1.154
12	26.9	21.7	267	12.3	1.91	1.94	1.502	22.7	20.9	228	10.89	2.00	2.03	1.259
13	27.0	21.5	251	11.6	1.80	1.83	1.636	22.7	21.2	223	10.52	1.93	1.96	1.367
14	26.8	21.7	255	11.8	1.83	1.86	1.729	22.7	21.0	218	10.36	1.90	1.93	1.475
15	26.9	21.7	248	11.4	1.77	1.79	1.888	22.7	21.2	214	10.09	1.87	1.89	1.577
16	26.9	21.6	245	11.4	1.76	1.79	2.02	22.7	21.2	214	10.12	1.86	1.88	1.692
17	26.9	21.9	247	11.3	1.75	1.78	2.15	22.7	21.0	210	9.98	1.83	1.85	1.801
18	26.9	21.8	242	11.1	1.72	1.75	2.27	22.7	21.1	206	9.78	1.79	1.82	1.905
19	26.9	21.7	238	10.9	1.69	1.73	2.40	22.7	21.1	208	9.85	1.81	1.83	2.01
20	26.9	21.8	245	11.3	1.75	1.78	2.52	22.6	21.0	205	9.77	1.80	1.83	2.11
21	26.8	22.0	234	10.6	1.66	1.68	2.65	22.6	21.1	202	9.57	1.76	1.79	2.22
22	26.9	22.0	218	9.92	1.55	1.58	2.79	22.6	21.5	190	9.85	1.64	1.66	2.32
23	26.9	22.2	229	10.3	1.60	1.63	2.92	22.7	21.5	195	9.05	1.66	1.69	2.44
	Nominal u_∞ = 54 ft/sec; t_∞ = 70.6° F; ρ_∞ = 0.0759 lb/cu ft							Nominal u_∞ = 43 ft/sec; t_∞ = 65.3° F; ρ_∞ = 0.0765 lb/cu ft						
2	14.8	21.1	296	14.04	3.96	4.02	0.115	11.7	16.6	165	9.95	3.53	3.57	0.092
3	14.7	21.7	235	10.83	3.06	3.11	.189	11.7	16.3	147	9.04	3.22	3.26	.151
4	14.8	21.7	210	9.66	2.72	2.76	.260	11.7	16.3	138	8.48	3.02	3.06	.206
5	14.8	21.9	201	9.18	2.59	2.63	.329	11.7	16.3	129	7.94	2.82	2.88	.264
6	14.7	21.9	195	8.92	2.52	2.57	.398	11.7	16.2	124	7.65	2.72	2.76	.319
7	14.7	21.8	188	8.61	2.44	2.48	.467	11.8	16.1	120	7.48	2.64	2.68	.377
8	14.8	21.8	185	8.46	2.38	2.43	.541	11.7	16.3	118	7.24	2.56	2.59	.433
9	14.8	22.0	190	8.63	2.44	2.48	.609	11.7	16.3	121	7.40	2.62	2.07	.489
10	14.8	22.1	175	7.92	2.24	2.28	.680	11.8	16.4	111	6.74	2.38	2.41	.546
11	14.8	21.9	168	7.67	2.16	2.20	.750	11.8	16.4	108	6.61	2.34	2.37	.601
12	14.9	21.9	172	7.86	2.20	2.24	.824	11.8	16.4	112	6.86	2.42	2.45	.660
13	14.8	22.0	167	7.58	2.14	2.17	.890	11.8	16.7	110	6.57	2.32	2.35	.715
14	14.8	21.7	164	7.55	2.13	2.16	.960	11.8	16.6	107	6.46	2.23	2.31	.771
15	14.8	22.0	163	7.43	2.09	2.13	1.033	11.8	16.4	109	6.67	2.35	2.38	.827
16	14.8	21.8	163	7.48	2.10	2.14	1.104	11.8	16.4	107	6.54	2.31	2.34	.884
17	14.8	21.8	149	7.30	2.00	2.10	1.169	11.8	16.9	108	6.38	2.26	2.29	.939
18	14.7	21.8	147	7.19	2.03	2.07	1.236	11.8	16.9	105	6.20	2.19	2.22	.995
19	14.8	21.9	153	7.00	1.97	2.01	1.310	11.7	16.9	102	6.01	2.13	2.16	1.048
20	14.8	21.9	153	6.99	1.96	1.99	1.382	11.8	16.7	101	6.07	2.14	2.17	1.104
21	14.7	22.1	156	7.07	2.00	1.97	1.440	11.7	16.8	104	6.17	2.19	2.22	1.160
22	14.8	22.2	141	6.35	1.79	1.82	1.518	11.7	16.6	93	5.58	1.98	2.02	1.214
23	14.8	22.4	148	6.59	1.86	1.89	1.589	11.7	16.9	99	5.84	2.07	2.10	1.270

TABLE I. - Concluded. EXPERIMENTAL DATA SUMMARY

(b) Velocity survey data

Distance from plate, y, in.	$Re_x = 0.731\times10^6$; $u_\infty = 41.2$ ft/sec; $\rho_\infty = 0.0770$ lb/cu ft	$Re_x = 0.970\times10^6$; $u_\infty = 40.9$ ft/sec; $\rho_\infty = 0.0771$ lb/cu ft	$Re_x = 1.210\times10^6$; $u_\infty = 40.4$ ft/sec; $\rho_\infty = 0.0782$ lb/cu ft	$Re_x = 1.738\times10^6$; $u_\infty = 99.6$ ft/sec; $\rho_\infty = 0.0755$ lb/cu ft	$Re_x = 2.32\times10^6$; $u_\infty = 99.1$ ft/sec; $\rho_\infty = 0.0757$ lb/cu ft	$Re_x = 2.91\times10^6$; $u_\infty = 97.8$ ft/sec; $\rho_\infty = 0.0760$ lb/cu ft
	Velocity ratio, u/u_∞					
0	0	0	0	0	0	0
.013	.405	.442	.370	.496	.511	.461
.015	.443	.456	.380	.498	.516	.466
.020	.506	.506	.445	.535	.532	.500
.025	.550	.538	.491	.559	.562	.534
.030	.578	.564	.520	.577	.577	.552
.035	-----	-----	-----	.590	.586	.568
.040	.598	.592	.551	.602	.598	.576
.045	-----	-----	-----	.616	.609	.588
.050	.632	.623	.580	.623	.616	.600
.060	.642	.634	.600	.646	.633	.616
.070	.659	.645	-----	.655	.648	.629
.080	.675	.655	.626	.671	.658	.640
.100	.702	.684	.641	.697	.682	.661
.125	.719	.698	.660	-----	-----	-----
.150	.750	.722	.679	.745	.722	.697
.175	.760	.731	.700	-----	-----	-----
.200	.778	.760	.716	.776	.752	.726
.250	.812	.778	.736	.814	.781	.752
.300	.848	.806	.772	.840	.806	.778
.350	.890	.845	.780	.874	.835	.801
.400	.896	.855	.718	.898	.857	.823
.450	.925	.885	.840	.920	.885	.841
.500	.950	.893	.855	.944	.902	.863
.550	.960	.924	.875	.960	.924	.882
.600	.962	.935	.893	.974	.938	.897
.650	.970	.957	.915	.984	.955	.915
.700	.972	.957	.927	.992	.968	.928
.750	.975	.964	.938	.996	.980	.942
.800	.988	.975	.952	1.000	.982	.956
.850	.994	.985	.958	1.000	.993	.971
.900	.999	.980	.974	1.000	.998	.977
.950	1.000	-----	.980	1.000	1.000	.992
1.000	1.000	.995	.990	1.000	1.000	.994
1.100	-----	1.000	1.000	-----	-----	-----

(c) Temperature survey data

$Re_x = 0.729\times10^6$		$Re_x = 0.978\times10^6$		$Re_x = 1.178\times10^6$		$Re_x = 1.72\times10^6$		$Re_x = 2.31\times10^6$		$Re_x = 2.78\times10^6$	
$t_w = t_\infty = 24.2^\circ$ F		$t_w - t_\infty = 24.9^\circ$ F				$t_w - t_\infty = 27.3^\circ$ F					
y, in.	θ	y, in.	θ	y, in.	θ	y, in.	θ	y, in.	θ	y, in.	θ
0	0	0	0	0	0	0	0	0	0	0	0
.004	.128	.004	.137	.005	.129	.003	.242	.004	.238	.004	.256
.005	.178	.005	.181	.006	.177	.004	.278	.005	.275	.005	.293
.006	.219	.006	.225	.007	.217	.006	.363	.007	.315	.007	.370
.007	.252	.007	.267	.008	.245	.008	.443	.009	.399	.009	.428
.008	.277	.008	.306	.009	.282	.010	.476	.011	.454	.011	.465
.009	.314	.009	.326	.010	.306	.012	.506	.013	.480	.013	.480
.010	.347	.010	.358	.011	.325	.014	.524	.015	.498	.015	.498
.011	.364	.011	.347	.012	.346	.016	.535	.017	.516	.017	.516
.013	.409	.013	.410	.014	.370	.018	.549	.019	.527	.019	.535
.015	.442	.015	.438	.016	.420	.023	.575	.024	.560	.024	.553
.017	.459	.017	.463	.018	.442	.028	.590	.029	.572	.029	.572
.019	.492	.019	.486	.020	.462	.033	.608	.034	.590	.034	.583
.021	.512	.021	.506	.024	.495	.038	.619	.039	.597	.039	.597
.023	.521	.023	.524	.029	.523	.043	.630	.044	.608	.044	.608
.028	.550	.028	.544	.034	.551	.048	.642	.049	.615	.049	.616
.033	.575	.033	.577	.044	.579	.058	.664	.059	.637	.059	.619
.043	.604	.043	.600	.054	.604	.068	.678	.069	.652	.069	.642
.053	.633	.053	.612	.064	.615	.078	.689	.079	.663	.079	.653
.063	.649	.063	.631	.074	.631	.098	.714	.099	.681	.099	.664
.073	.666	.073	.651	.084	.648	.148	.754	.149	.722	.149	.708
.083	.678	.083	.660	.104	.668	.198	.795	.199	.754	.199	.736
.103	.703	.103	.680	.154	.704	.248	.827	.249	.792	.249	.755
.153	.748	.153	.720	.204	.728	.298	.865	.299	.817	.299	.784
.203	.790	.203	.775	.254	.760	.348	.890	.349	.842	.349	.806
.253	.823	.253	.792	.304	.788	.398	.912	.399	.864	.399	.825
.303	.847	.303	.816	.354	.806	.448	.934	.449	.883	.449	.846
.353	.876	.353	.840	.404	.825	.498	.955	.499	.902	.499	.865
.403	.909	.403	.864	.504	.864	.548	.974	.549	.924	.599	.902
.503	.950	.503	.905	.604	.905	.598	.989	.599	.941	.699	.930
.603	.988	.603	.945	.704	.921	.648	.999	.649	.956	.799	.963
.703	.988	.703	.973	.804	.960	.698	1.000	.699	.978	.899	.981
.803	.996	.803	.996	.904	.977	.798	1.000	.799	.996	.999	.996
.903	1.000	.903	1.000	1.004	.997	.898	1.000	.899	1.000	1.099	1.000

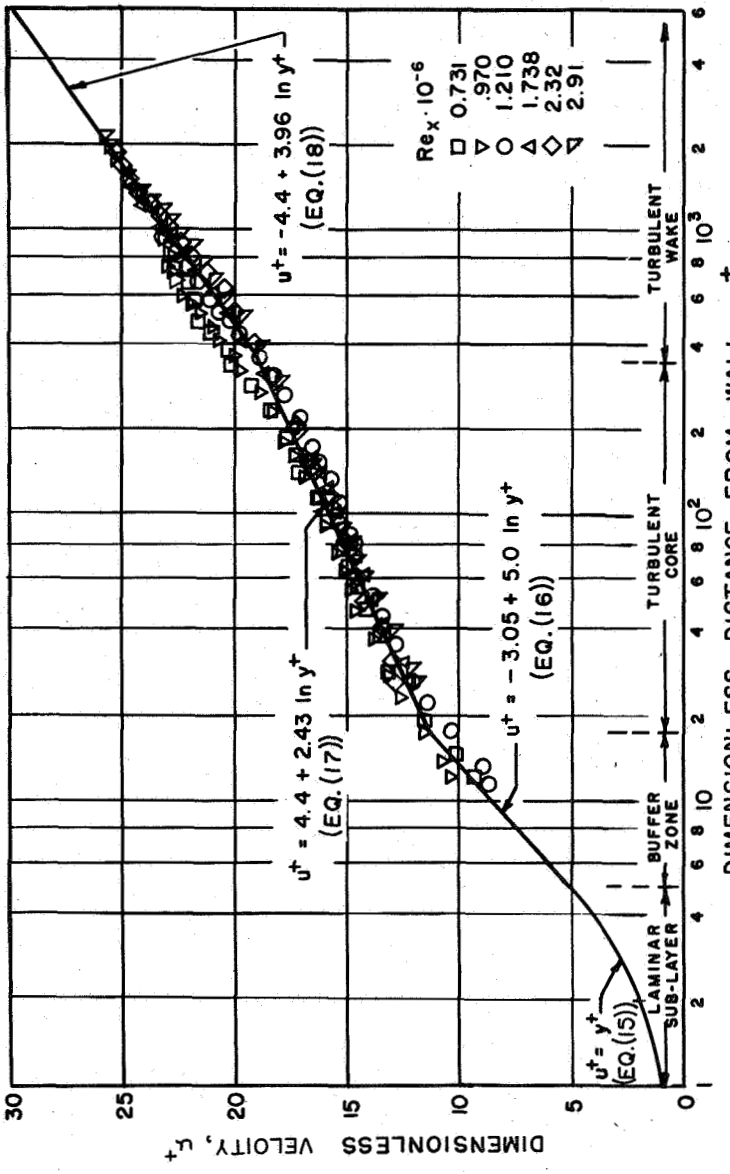

Figure 1. - Comparison of universal flat-plate velocity profile with experimental data.

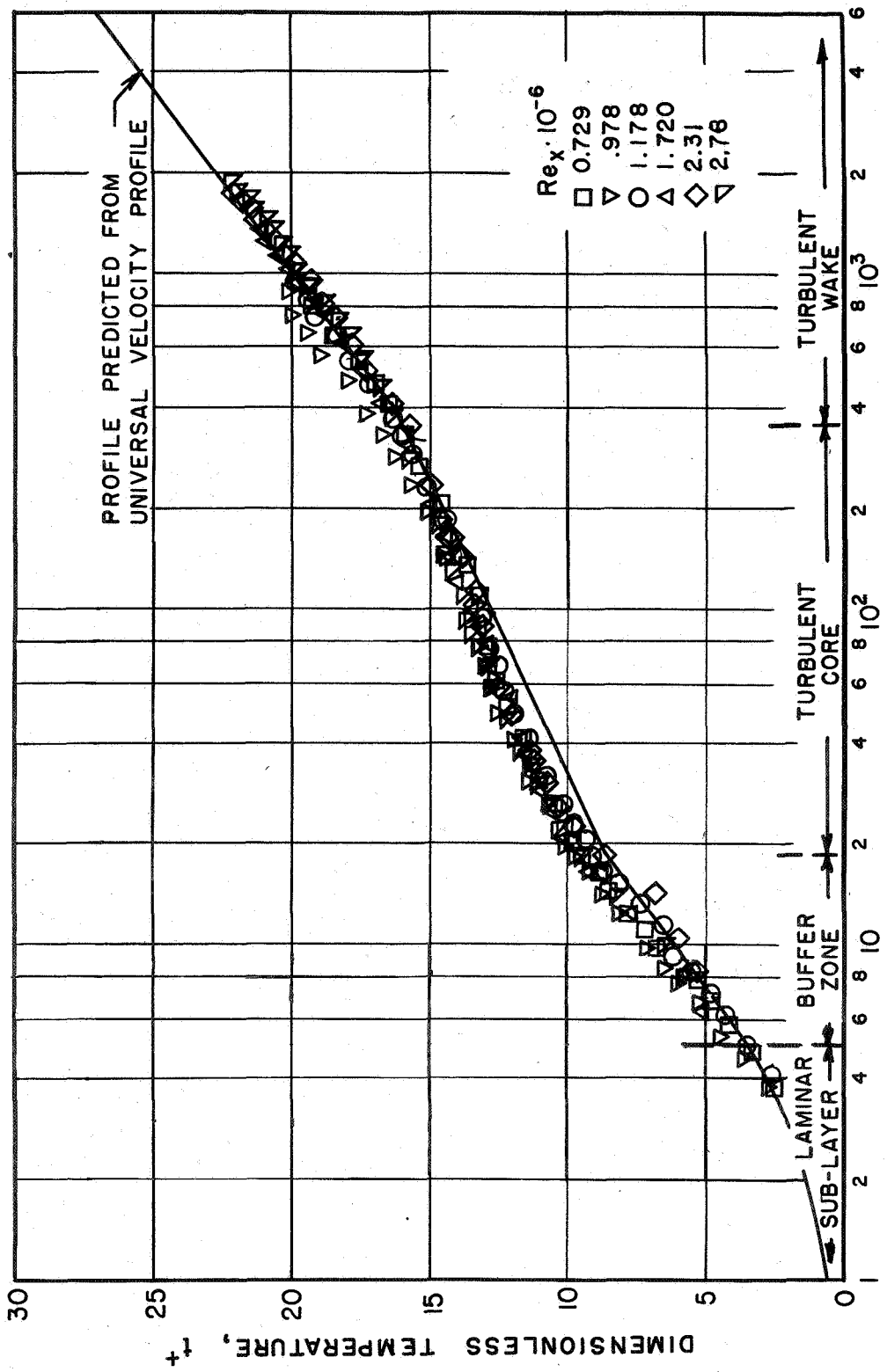

Figure 2. - Universal flat-plate temperature profile. Prandtl number, 0.7.

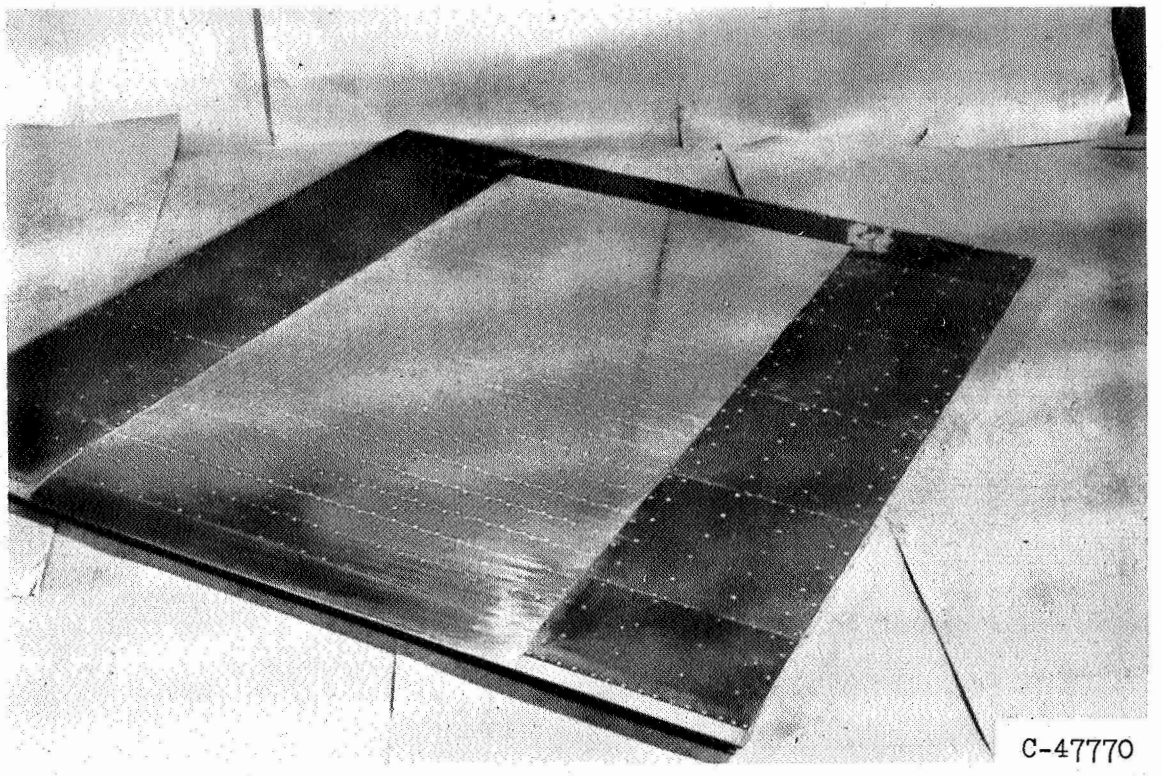

(a) Plate before mounting.

Figure 3. - Experimental flat plate.

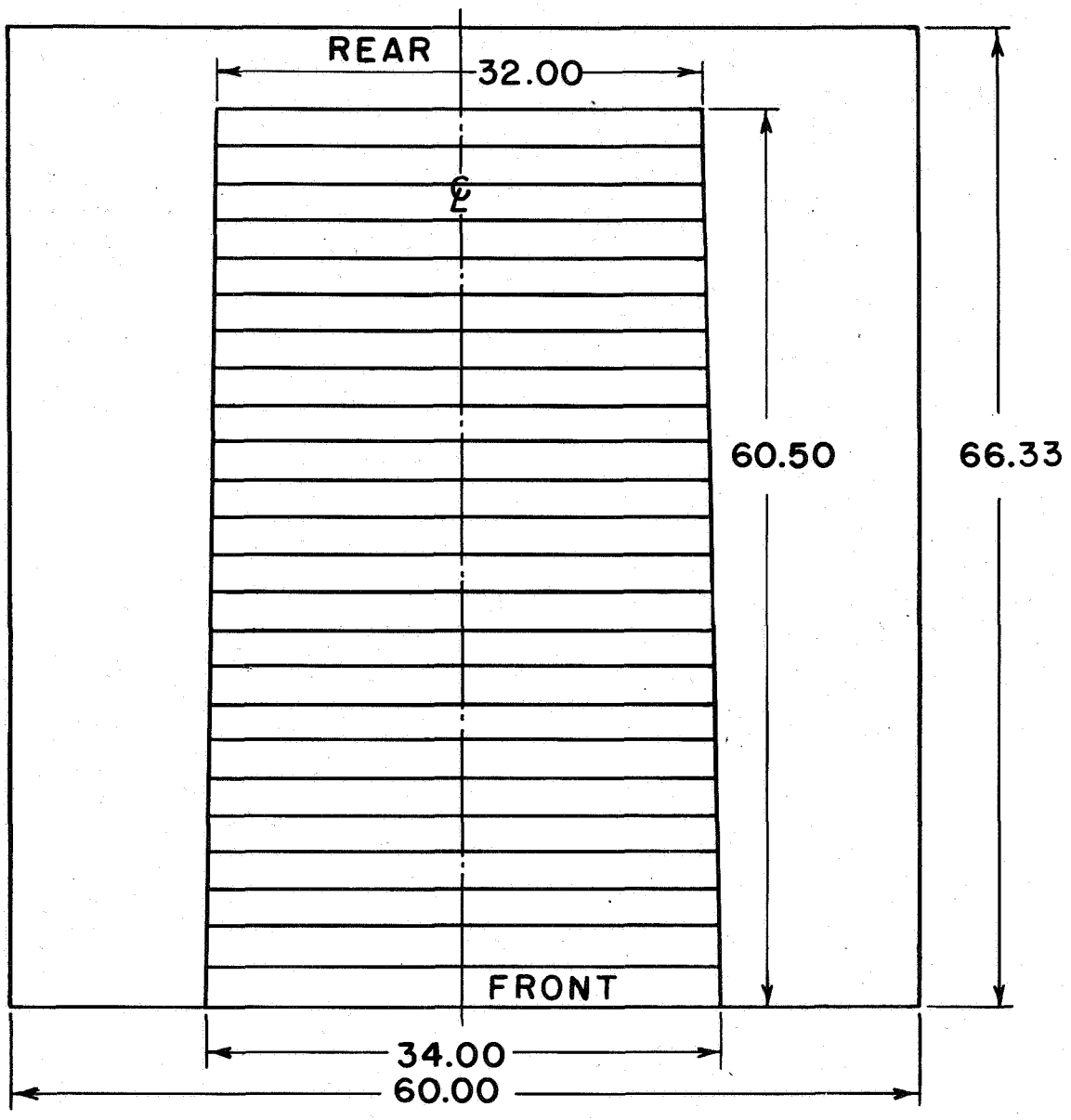

(b) Plan view showing heated-section dimensions (in inches).

Figure 3. - Concluded. Experimental flat plate.

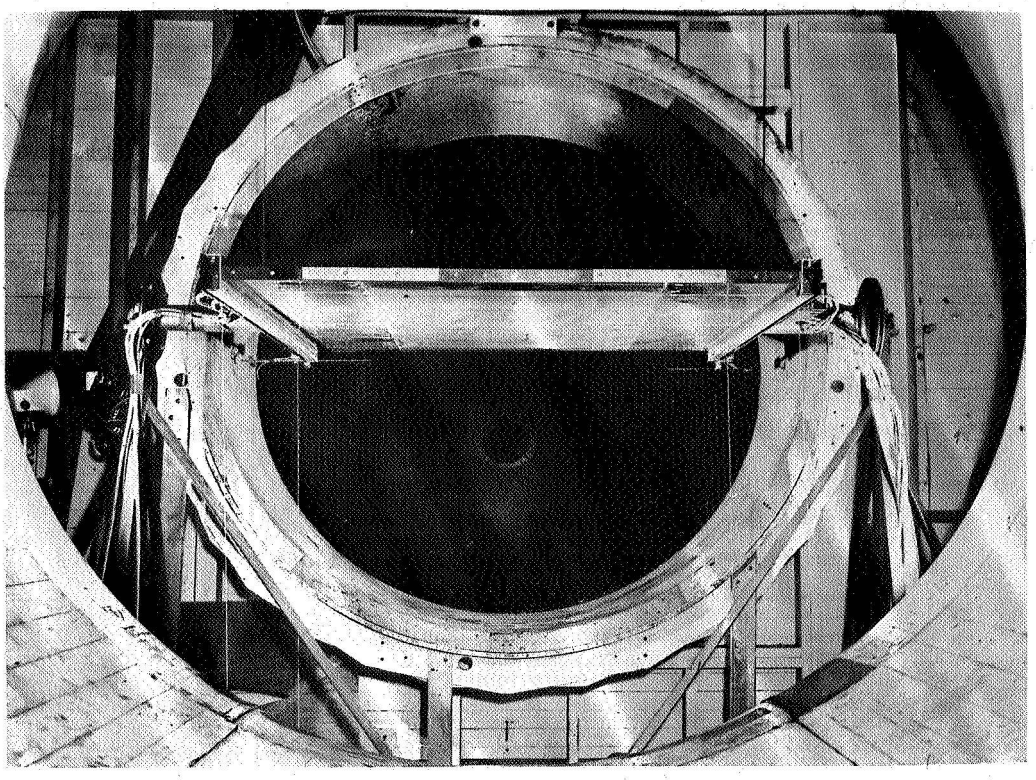

(a) View from inside of downstream collector.

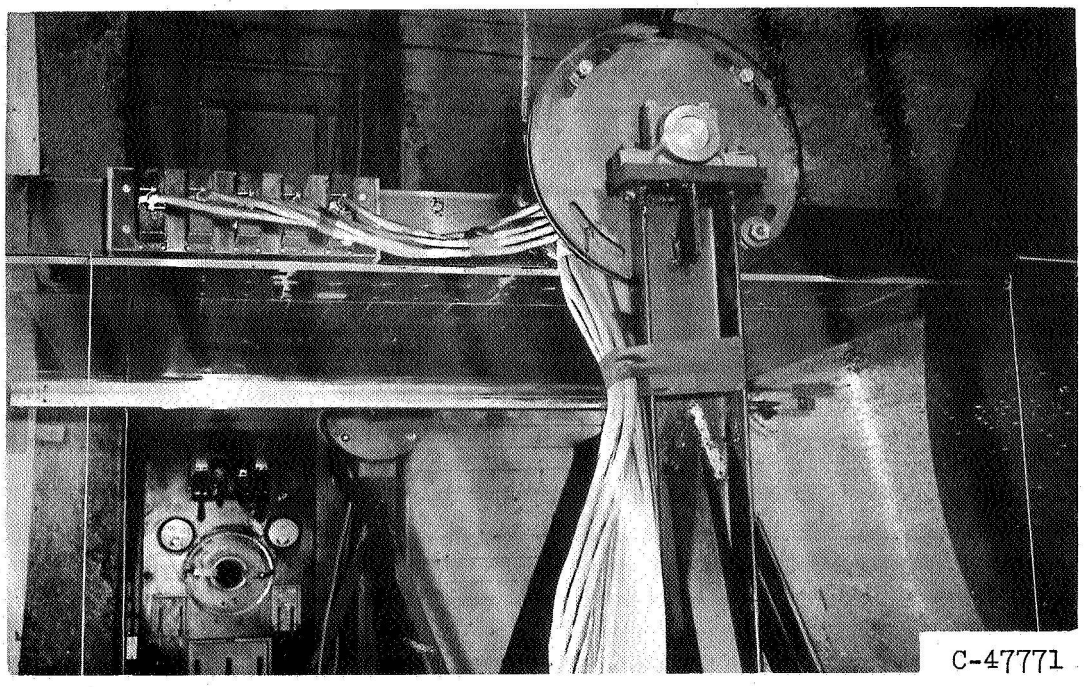

(b) Side view.

Figure 4. - Wind-tunnel installation.

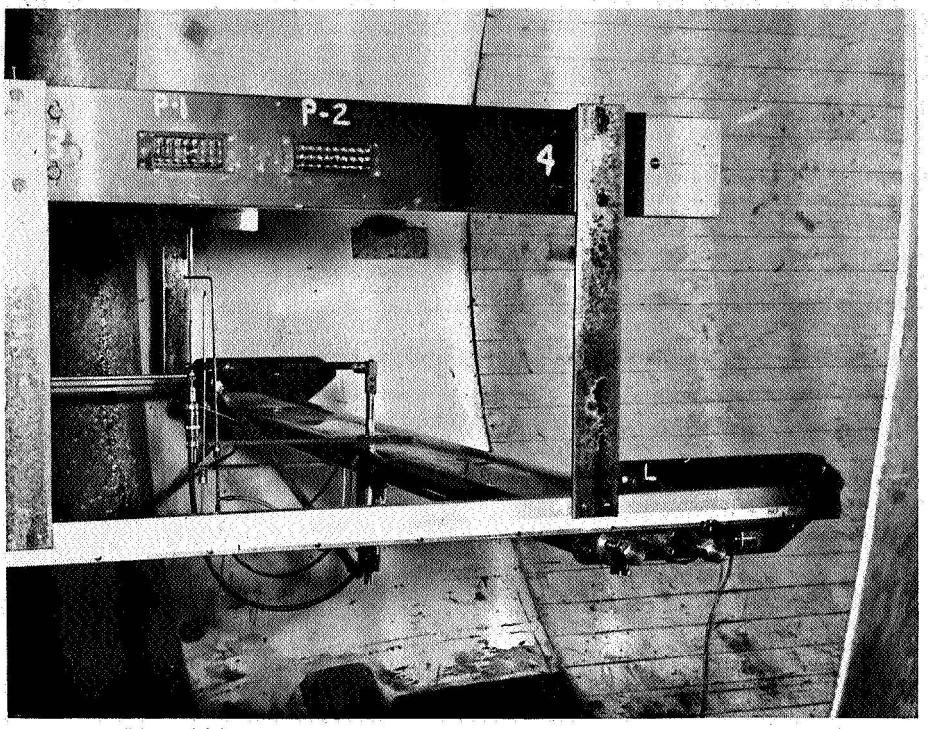

(c) Traverse mechanism.

Figure 4. - Concluded. Wind-tunnel installation.

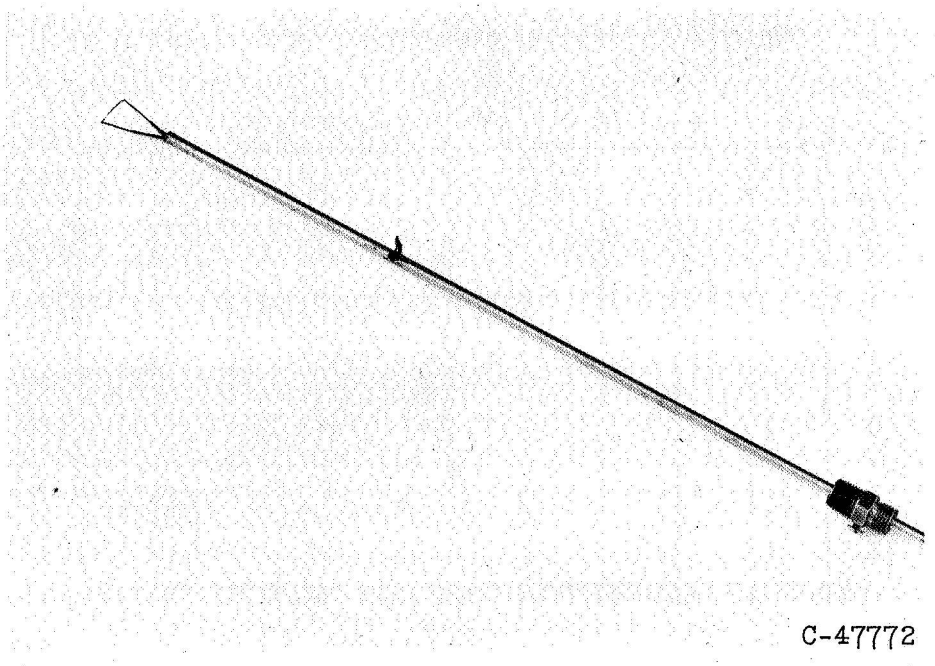

Figure 5. - Thermocouple probe.

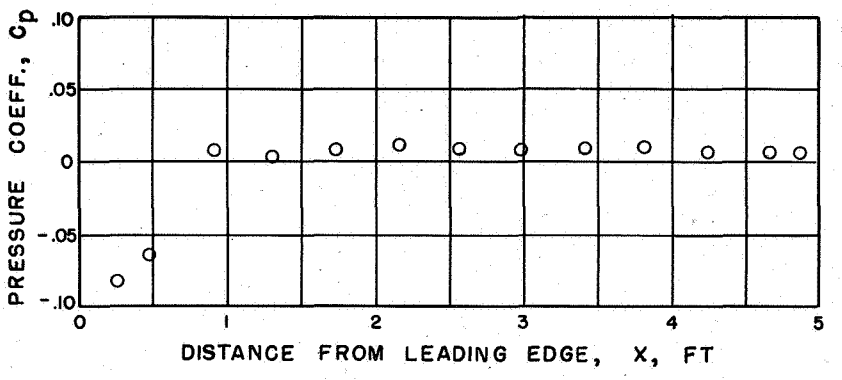

(a) Longitudinal.

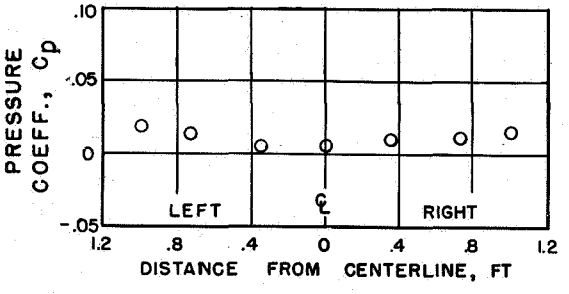

(b) Transverse; x = 4.65 feet.

Figure 6. - Typical pressure distributions.

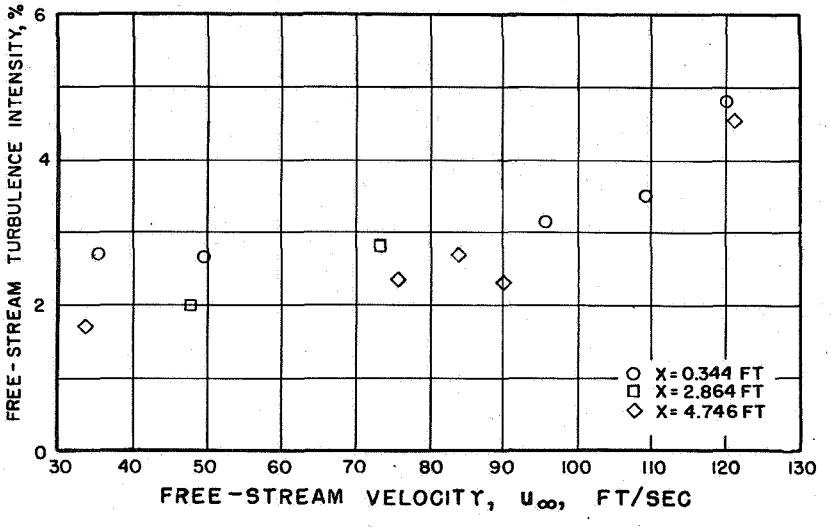

Figure 7. - Free-stream turbulence intensity.

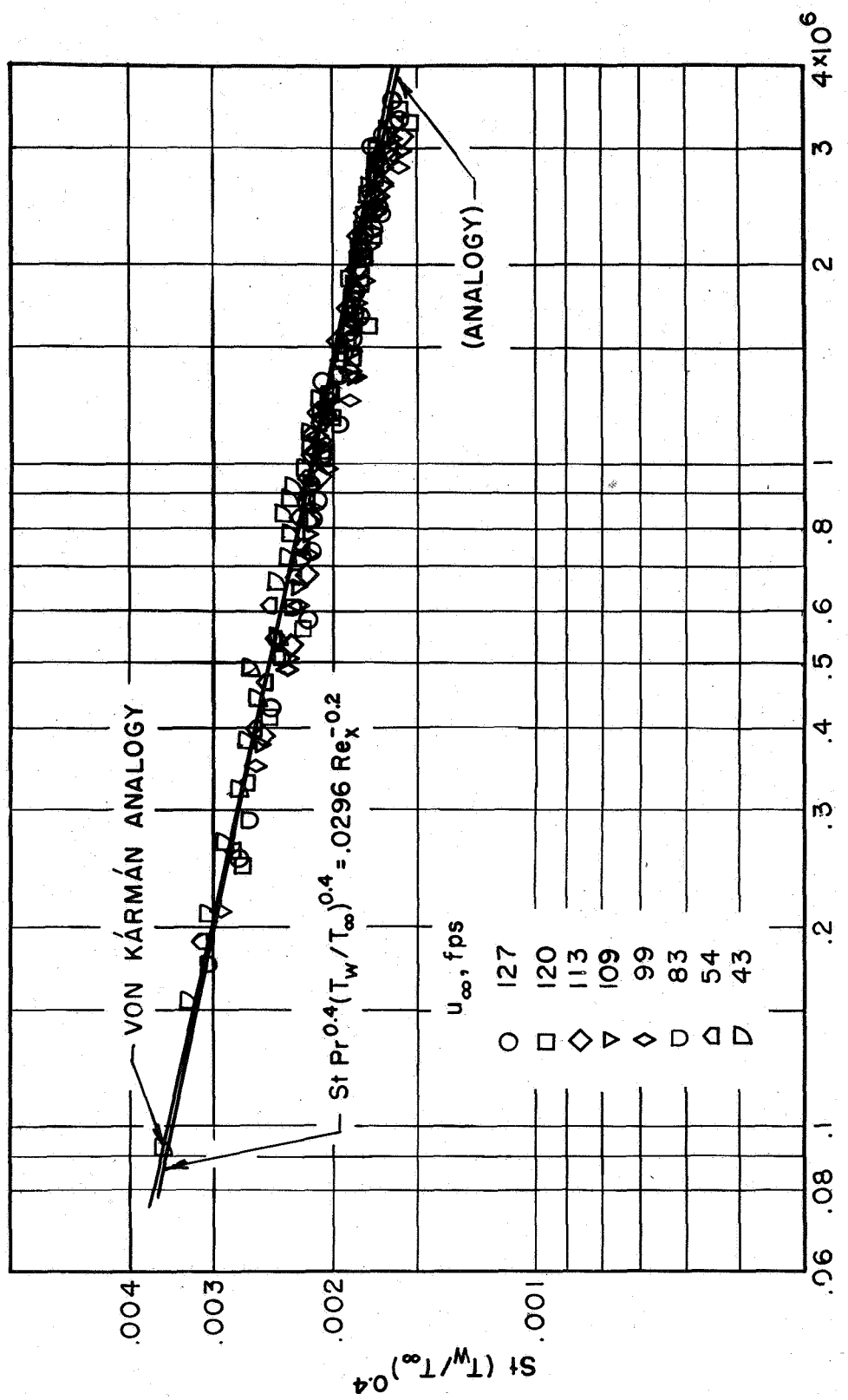

Figure 8. - Local Stanton numbers for constant temperature. Prandtl number, 0.7.

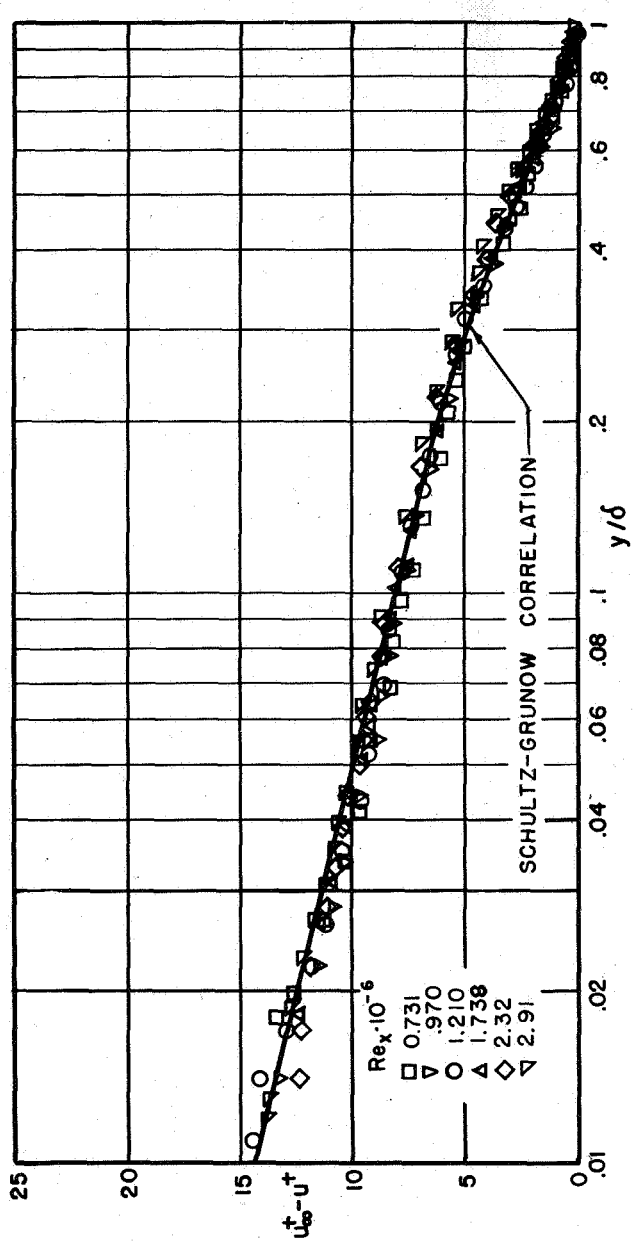

Figure 9. - Comparison of velocity surveys with Schultz-Grunow profile.

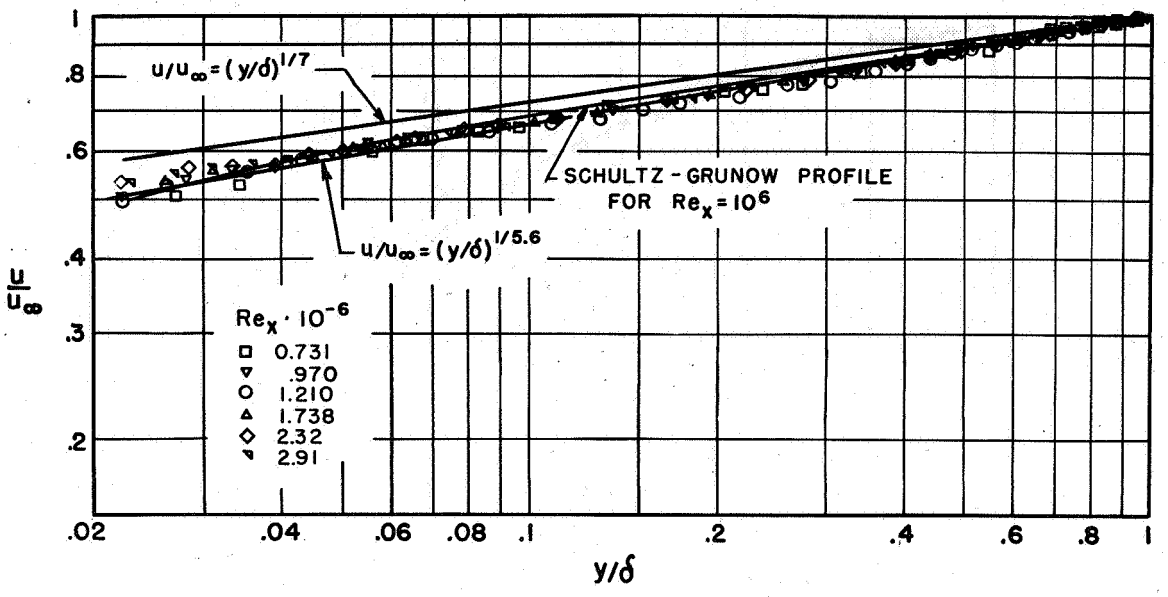

(a) Variation of u/u_∞ with y/δ.

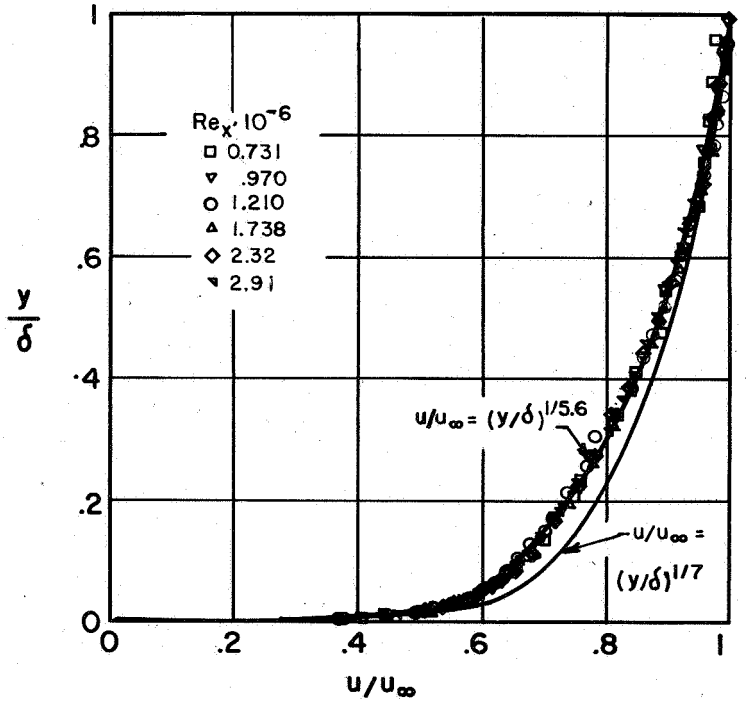

(b) Variation of y/δ with u/u_∞.

Figure 10. - Turbulent velocity profiles.

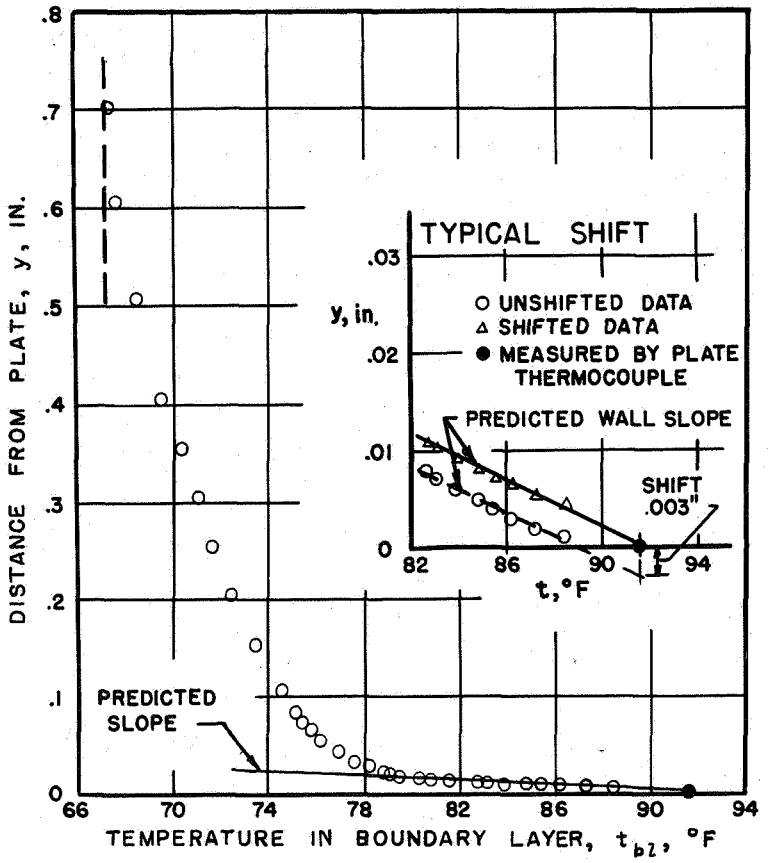

Figure 11. - Typical temperature survey.

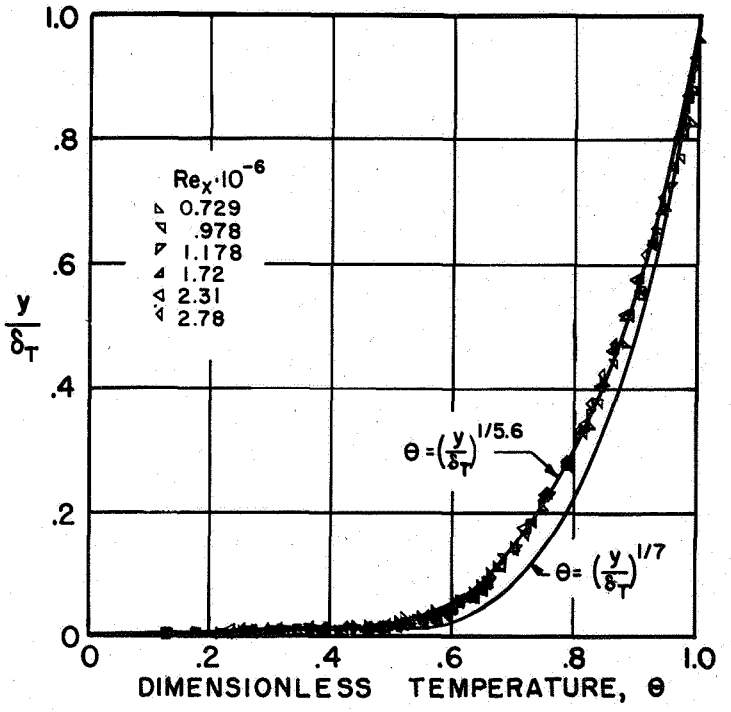

Figure 12. - Temperature profiles for constant surface temperature.